Editors' Suggestion

Temperature effect on charge-state transition levels of defects in semiconductors

Shuang Qiao,[1] Yu-Ning Wu,[2] Xiaolan Yan,[1] Bartomeu Monserrat,[3,4] Su-Huai Wei,[1,5] and Bing Huang[1,5,*]

[1]*Beijing Computational Science Research Center, Beijing 100193, China*

[2]*Key Laboratory of Polar Materials and Devices (MOE) and Department of Electronics, East China Normal University, Shanghai 200241, China*

[3]*Cavendish Laboratory, University of Cambridge, Cambridge CB3 0HE, United Kingdom*

[4]*Department of Materials Science and Metallurgy, University of Cambridge, Cambridge CB3 0FS, United Kingdom*

[5]*Department of Physics, Beijing Normal University, Beijing 100875, China*

(Received 8 October 2021; accepted 24 February 2022; published 8 March 2022)

Defects are crucial in determining the overall physical properties of semiconductors. Generally, the charge-state transition level $\varepsilon_\alpha(q/q')$, one of the key physical quantities that determines the dopability of defects in semiconductors, is temperature dependent. However, little is known about the temperature dependence of $\varepsilon_\alpha(q/q')$ and, as a result, almost all existing defect theories in semiconductors are built on a temperature-independent approximation. In this paper, by deriving the basic formulas for temperature-dependent $\varepsilon_\alpha(q/q')$, we have established two fundamental rules for the temperature dependence of $\varepsilon_\alpha(q/q')$ in semiconductors. Based on these rules, surprisingly, it is found that the temperature dependencies of $\varepsilon_\alpha(q/q')$ for different defects are rather diverse: it can become shallower, deeper, or stay unchanged. This defect-specific behavior is mainly determined by the synergistic or opposing effects between free-energy corrections (determined by the local volume change around the defect during a charge-state transition) and band-edge changes (which differ for different semiconductors). These basic formulas and rules, confirmed by a large number of state-of-the-art temperature-dependent defect calculations in GaN, may potentially be widely adopted as guidelines for understanding or optimizing doping behaviors in semiconductors at finite temperatures.

DOI: 10.1103/PhysRevB.105.115201

I. INTRODUCTION

Intrinsic defects and external impurities (generally denoted as defects hereafter) play a critical role in determining the physical properties of solids, e.g., from solar cells [1–3] to solid-state lighting [4,5] to topological phase control [6–8] and to quantum computing [9–11]. The defect formation energies $H_f(\alpha,q)$ for defect α at charge state q that determine the defect concentrations and the charge-state transition levels $\varepsilon_\alpha(q/q')$ that correspond to the thermal ionization energies are two of the most important physical quantities for all the defects in semiconductors [12–14]. Generally, both $H_f(\alpha,q)$ and $\varepsilon_\alpha(q/q')$ are temperature dependent. Differing from the straightforward temperature dependence of $H_f(\alpha,q)$ [12,13,15–17], little is known about how temperature changes affect $\varepsilon_\alpha(q/q')$ in semiconductors due to the lack of basic formulas and fundamental rules. As a result, almost all defect theories in semiconductors are built on static first-principles calculations excluding temperature effects [12–14].

The challenge to unravel the temperature dependence of $\varepsilon_\alpha(q/q')$ in theory is twofold. Fundamentally, the standard formulas for $\varepsilon_\alpha(q/q')$ calculations are incomplete and do not capture the $\varepsilon_\alpha(q/q')$ of defects under finite temperatures. Practically, the computations of temperature-induced vibrational properties of defects in semiconductors are rather expensive. Because of its unparalleled complexity, the temperature dependence of $\varepsilon_\alpha(q/q')$ in semiconductors has remained unanswered for decades, i.e., we do not have any available rules to predict or understand the dopability of semiconductors at finite or changing temperatures.

Differing from narrow band gap (NBG) semiconductors (e.g., Si and GaAs) that usually operate under ambient environments at room temperature, wide band gap (WBG) semiconductors (e.g., GaN and SiC) can operate under harsh environments with high working temperatures [18–22]. Therefore, WBG semiconductors are an ideal platform for unique applications in aerospace, nuclear power, and earth's mantle investigations that require changing operation temperatures from extremely low to extremely high (0∼1000 K) [18–26]. This highlights the need to understand the evolution with temperature of defect properties in WBG semiconductors, especially of $\varepsilon_\alpha(q/q')$, which may be critical to improve the reliability of WBG semiconductor devices in various environments.

In this paper, by deriving the basic formulas of temperature-dependent $\varepsilon_\alpha(q/q')$, we have established two fundamental rules for the temperature dependence of absolute and relative $\varepsilon_\alpha(q/q')$ in semiconductors, respectively. Based on these rules, it is found that regardless of the initial $\varepsilon_\alpha(q/q')$ levels at 0 K, surprisingly, the temperature-dependent behaviors of $\varepsilon_\alpha(q/q')$ for different defects in different types of semiconductors are rather diverse, i.e., it can become shallower, deeper, or even stay unchanged, mainly determined by

*Bing.Huang@csrc.ac.cn

the synergistic or opposing effects between free-energy corrections and band-edge changes. Importantly, we discover that the electronic and vibrational contributions to free-energy corrections are both fundamentally determined by a key physical quantity $\delta V_{q\to q'}$, the local volume change around the defect during the charge-state transition. Interestingly, the $\delta V_{q\to q'}$ values are mainly determined by the competing effect between the local electron occupation (LEO) changes and the strength of the local lattice relaxation (LLR) around the defects. Using the state-of-art first-principles-based temperature-dependent approaches with the capacity of both high accuracy and high efficiency [27], these proposed basic formulas and fundamental rules have been thoroughly verified based on a large number of defect calculations in GaN.

II. RESULTS AND DISCUSSION

A. Basic formulas

Without the inclusion of temperature effects, the ε_α(q/q') of defect α between the charge states q and q' is given as

$$\varepsilon_\alpha(q/q')_{w.o.T} = \frac{E(\alpha, q') - E(\alpha, q)}{q - q'} - \varepsilon_{\mathrm{VBM}}(host), \quad (1)$$

where E(α,q) [E(α,q')] is the total energy of a supercell with defect α in charge state q [q'] and $\varepsilon_{\mathrm{VBM}}$(host) is the valence band maximum (VBM) of the host [12–14]. With the inclusion of temperature effects, E(α,q) [E(α,q')] in Eq. (1) is replaced by the corresponding free energy F(α,q) [F(α,q')]. After some manipulations (see Appendix A), it can be written as

$$\varepsilon_\alpha(q/q')[V,T] = \varepsilon_\alpha(q/q')_{w.o.T} + \frac{\Delta F^{\mathrm{el}}[V,T] + \Delta F^{\mathrm{ph}}[V,T]}{q - q'} - \Delta\varepsilon_{\mathrm{VBM}}(\mathrm{host})[V,T]. \quad (2)$$

On the right-hand side of Eq. (2), the second term represents the corrections from the free-energy differences between the q and q' configurations induced by the electronic (ΔF^{el}) and vibrational (ΔF^{ph}) contributions, while the third term represents the correction on the VBM energy position driven by thermal expansion and electron-phonon coupling ($\Delta\varepsilon_{\mathrm{VBM}} = \Delta\varepsilon^{\mathrm{th}}{}_{\mathrm{VBM}} + \Delta\varepsilon^{\mathrm{ph}}_{\mathrm{VBM}}$). While the temperature should affect both the band edges and formation energies [ε_α(q/q')] at the same time, as shown in Eq. (2), at the impurity limit as modeled, it is rigorous to consider the temperature effect on free-energy differences and band-edge changes separately. Specifically, the band-edge shift is calculated based on the evaluation of electron-phonon coupling and thermal expansion, whereas the correction of formation energies (including ΔF^{el} and ΔF^{el}) comes from the Gibbs free energy. The coupling of these corrections at the impurity limit is negligible. In addition, for magnetic defects, the magnetic contributions to formation enthalpy and entropy should also be included.

In practice, the temperature dependence of ε_α(q/q') can be understood without and with the inclusion of $\Delta\varepsilon_{\mathrm{VBM}}$ [28], corresponding to the absolute and relative evolutions of ε_α(q/q'), respectively. Here, relative means relative to the VBM(T) at a given temperature T, while absolute refers to an absolute energy scale [reference to vacuum or VBM(T = 0)]. While the temperature dependence of the absolute ε_α(q/q') [ε^a_α(q/q')] is solely determined by the free-energy corrections, that of the relative ε_α(q/q') [ε^r_α(q/q')] is determined by both the free-energy corrections and the band-edge changes. Although ε_α(q/q') is independent of the direction of charge-state transitions, to simplify our discussion, in the following we focus on the ionization process, i.e., |q'| > |q|. This assumption does not change the rules we developed.

Under the quasiharmonic approximation (QHA), F^{el} can be written as $F^{\mathrm{el}} = E^{\mathrm{th}}+E^{\mathrm{el}}\text{-}TS^{\mathrm{el}}$ [13,29,30], where the first, second, and third terms are the energy corrections induced by thermal expansion, electron-occupation change, and electronic entropy, respectively. Generally, the contributions from E^{el} and S^{el} to F^{el} are negligible under reasonable temperatures in semiconductors [12,31] (also see more explanation in Appendix A). Therefore, we focus on the E^{th} term in F^{el}. Without an external pressure, $V = \varphi_V\, T\, V_0 + V_0$, where φ_V is the mean volumetric thermal expansion coefficient (usually, $\varphi_V > 0$) and V_0 is the equilibrium volume at 0 K. Ignoring high order terms (see Appendix B), ΔE^{th} can be expressed as

$$\Delta E^{\mathrm{th}} = -2\gamma_0\, \varphi_V T\, V_0(\mathrm{host})\, \delta V_{q\to q'}. \quad (3)$$

Here, γ_0 is the elastic constant and $\delta V_{q\to q'}$ is defined as the local volume change during the ionization of defect α from q to q'. It can be approximately estimated by $\delta V_{q\to q'} = V_0(\alpha,q')\text{-}V_0(\alpha,q)$, where $V_0(\alpha,q')$ and $V_0(\alpha,q)$ are the volumes of the fully optimized supercells with defect α under q and q' charge states, respectively.

Moving to F^{ph}, it can be expressed as $F^{\mathrm{ph}} = \sum_i[\frac{1}{2}\hbar\omega_i + k_B T \ln\{1\text{-}\exp(\text{-}\frac{\hbar\omega_i}{k_B T})\}]$ under the QHA [32], where $\hbar$, ω_i, and k_B are the reduced Planck's constant, phonon eigenfrequency, and Boltzmann constant, respectively. Consequently, under a first-order approximation (see Appendix C), ΔF^{ph} can be written as

$$\Delta F^{\mathrm{ph}} = \Delta F^{\mathrm{zp}} + \Delta\widetilde{F}^{\mathrm{ph}} = \sum_i \frac{1}{2}\hbar\Delta\omega_i + \sum_i k_B T \frac{\Delta\omega_i}{\omega_i(\alpha, q)}, \quad (4)$$

where $\Delta\omega_i = \omega_i(\alpha,q')\text{-}\omega_i(\alpha,q)$ is the ith phonon eigenfrequency difference for defect α during the ionization from q to q'. ΔF^{zp} is the contribution of zero-point vibrations and the $\Delta\widetilde{F}^{\mathrm{ph}}$ is the pure temperature-dependent part.

B. Fundamental rules

First, we consider the role of ΔF^{el} (dominated by ΔE^{th}) on ε_α(q/q'). In a common semiconductor, rising temperature leads to volume expansion ($\varphi_V > 0$). During the ionization of an acceptor from q to q', the $\delta V_{q\to q'}$ of the defect may expand due to the increased electron occupation, giving rise to a positive $\delta V_{q\to q'}$. Oppositely, for a donor, the $\delta V_{q\to q'}$ may shrink due to the reduced electron occupation during the ionization, giving rise to a negative $\delta V_{q\to q'}$. According to Eq. (3), ΔE^{th} is negative and decreases with increasing temperature for an acceptor, shallowing ε_α(q/q'); ΔE^{th} is positive and increases with increasing temperature for a donor, deepening ε_α(q/q').

Second, we consider the role of ΔF^{ph} on ε_α(q/q'). According to Eq. (4), the sign of ΔF^{ph} is mostly determined by $\Delta\omega_i$. The phonon frequencies can be approximately understood using a one-dimensional harmonic oscillator model with $\omega \sim \sqrt{\frac{k}{m}}$, where k is the force constant for the system, capturing

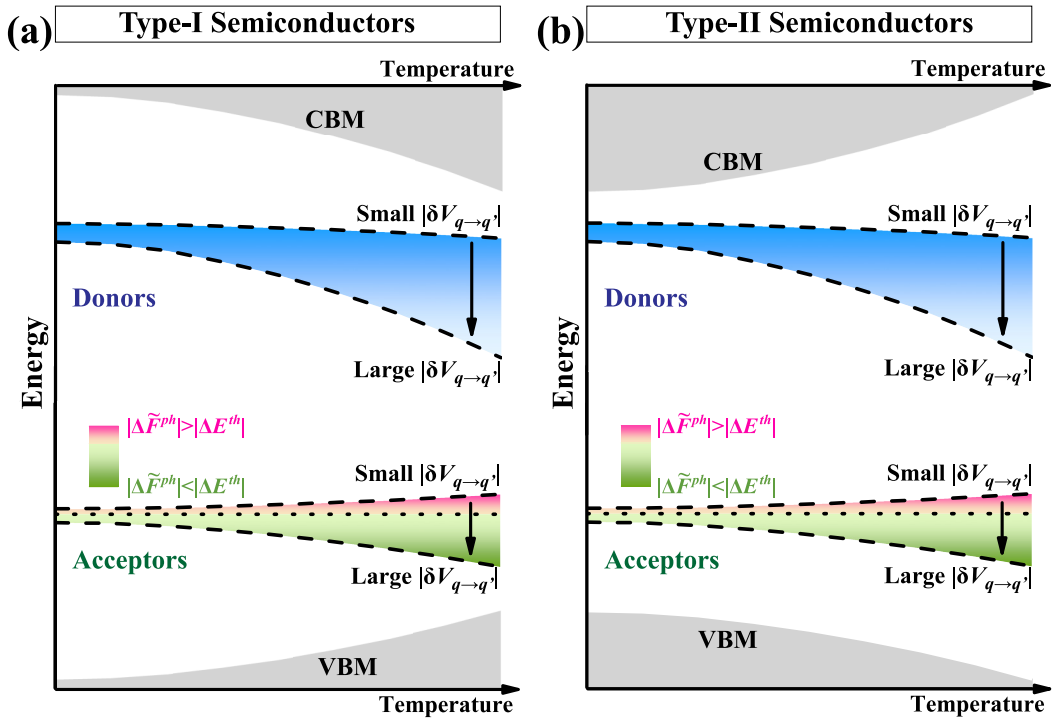

FIG. 1. Fundamental rules for temperature-dependence of $\varepsilon_\alpha(q/q')$. Schematic illustration of the effects of temperature on $\varepsilon_\alpha(q/q')$ levels in (a) type-I and (b) type-II semiconductors, in which $|\delta V_{q\to q'}|$ is discovered to play a critical role. For convenience of plotting, we assume that donors (or acceptors) have similar $\varepsilon_\alpha(q/q')$ at 0 K [note that $\Delta\varepsilon_\alpha(q/q')$ is independent of the initial $\varepsilon_\alpha(q/q')$ at 0 K]. See text for more details.

the strength of atomic bonds. During the ionization of both acceptor and donor, the bond strength around the defect could be enhanced because the number of electrons on the chemical bonds are closer to the host chemical bonds. Therefore, $\Delta\omega_i$ is positive for both donors and acceptors. Consequently, ΔF^{ph} is positive and increases with rising temperature, deepening $\varepsilon_\alpha(q/q')$ for both donors and acceptors. Moreover, it is expected that $\delta V_{q\to q'}$ and $\bar{m}$ (defined as the average atomic mass of the defect and its nearest-neighbor atoms) may be key factors in determining the exact value of ΔF^{ph}. Specifically, a larger $\delta V_{q\to q'}$ indicates a larger bonding strength change around the defect during the charge-state transition, leading to the larger $\Delta\omega_i$ (and hence larger ΔF^{ph}); the larger the $\bar{m}$, the smaller the ΔF^{zp}.

Based on the above understanding of ΔF^{el} and ΔF^{ph}, we can propose two fundamental rules for the temperature dependence of $\varepsilon^a_\alpha(q/q')$ and $\varepsilon^r_\alpha(q/q')$, respectively. For donors, both ΔF^{el} and ΔF^{ph} can downshift the $\varepsilon^a_\alpha(q/q')$ levels toward lower energy values, and the downshift grows with temperature. Meanwhile, as shown in Fig. 1, the larger the $|\delta V_{q\to q'}|$ of a donor, the larger the ΔE^{th} and ΔF^{ph} and, consequently the larger the downshift of $\varepsilon^a_\alpha(q/q')$. For acceptors, the (negative) ΔF^{el} and (positive) ΔF^{ph} have a canceling effect, because they cause the $\varepsilon^a_\alpha(q/q')$ level to shift in opposite directions. Comparing Eqs. (3) and (4), it is expected that the changes of $|\Delta E^{th}|$ could be more significant than those of $|\Delta\widetilde{F}^{ph}|$ for the variable $|\delta V_{q\to q'}|$. Accordingly, as shown in Fig. 1, for an acceptor with small $|\delta V_{q\to q'}|$, $|\Delta\widetilde{F}^{ph}| > |\Delta E^{th}|$, which may upshift $\varepsilon^a_\alpha(q/q')$ in energy; for an acceptor with large $|\delta V_{q\to q'}|$, $|\Delta\widetilde{F}^{ph}| < |\Delta E^{th}|$, which may downshift $\varepsilon^a_\alpha(q/q')$ in energy. Therefore, we can propose rule I on the changes of $\varepsilon^a_\alpha(q/q')$ $[\Delta\varepsilon^a_\alpha(q/q')]$ in semiconductors at different temperatures. *Rule I(a) for donors:* The higher the temperature, the larger the $\Delta\varepsilon^a_\alpha(q/q')$ toward deeper levels; the larger the $|\delta V_{q\to q'}|$, the larger the $\Delta\varepsilon^a_\alpha(q/q')$ toward deeper levels. *Rule I(b) for acceptors:* For the acceptors with large $|\delta V_{q\to q'}|$, the higher the temperature, the larger the $\Delta\varepsilon^a_\alpha(q/q')$ toward shallower levels; the larger the $|\delta V_{q\to q'}|$, the larger the $\Delta\varepsilon^a_\alpha(q/q')$ toward shallower levels; for acceptors with small $|\delta V_{q\to q'}|$, the higher the temperature, the larger the $\Delta\varepsilon^a_\alpha(q/q')$ toward deeper levels; the smaller the $|\delta V_{q\to q'}|$, the larger the $\Delta\varepsilon^a_\alpha(q/q')$ toward deeper levels.

After having established the role of the free-energy corrections, we next consider the changes in the band edge. Generally, for most conventional semiconductors, there are two typical types of temperature-dependent band edge changes, as demonstrated in Fig. 1. In many conventional semiconductors, e.g., GaN [33,34] and GaAs [35], the CBM energy positions usually downshift, while the VBM energy positions upshift as temperature increases, e.g., $\Delta\varepsilon_{CBM} < 0$ and $\Delta\varepsilon_{VBM} > 0$, denoted as type-I semiconductors [Fig. 1(a)]. Type-II semiconductors [Fig. 1(b)], e.g., $CsPbI_3$ [36] and $MAPbI_3$ [37,38], are opposite to the type-I cases, e.g., $\Delta\varepsilon_{CBM} > 0$ and $\Delta\varepsilon_{VBM} < 0$. Combining Rule I and specific band-edge changes, we arrive at rule II on the temperature dependence of $\varepsilon^r_\alpha(q/q')$ in semiconductors. *Rule II(a) for donors:* The $\varepsilon^r_\alpha(q/q')$ in type-I semiconductors can become shallower, deeper, or stay unchanged under different temperatures [Fig. 1(a)], depending on the different strengths of the opposing effect between $\Delta\varepsilon^a_\alpha(q/q')$ and $\Delta\varepsilon_{CBM}$; the $\varepsilon^r_\alpha(q/q')$ in type-II semiconductors will always become deeper (Fig. 1(b)), due to the synergistic effect between $\Delta\varepsilon^a_\alpha(q/q')$ and $\Delta\varepsilon_{CBM}$. *Rule II(b) for acceptors:* The $\varepsilon^r_\alpha(q/q')$ with small $|\delta V_{q\to q'}|$ in

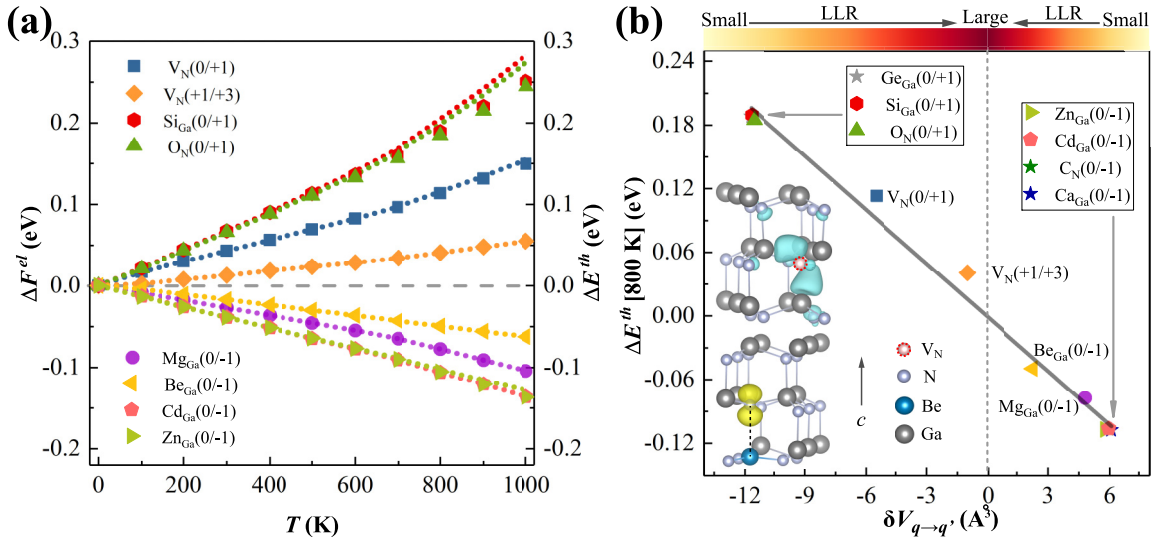

FIG. 2. Electronic contribution to the temperature dependence of ε_α(q/q') in GaN. (a) ΔF^{el} (dashed lines) and ΔE^{th} (symbols) as a function of temperature for different defects in GaN. (b) Relationship between $\delta V_{q\to q'}$ and ΔE^{th} for different defects at 800 K. Up inset and bottom inset are partial charge densities for neutral V_N and Be_{Ga}, respectively. Black-dashed line in the bottom inset shows the broken bond between Be and its neighboring *N*.

type-I semiconductors and the ε^r_α(q/q') with large $|\delta V_{q\to q'}|$ in type-II semiconductors can become either shallower, deeper, or stay unchanged as a function of temperature, originating from the opposing effect between $\Delta\varepsilon^a_\alpha$(q/q') and $\Delta\varepsilon_{\rm VBM}$; the ε^r_α(q/q') with large $|\delta V_{q\to q'}|$ in type-I semiconductors and the ε^r_α(q/q') with small $|\delta V_{q\to q'}|$ in type-II semiconductors will always become shallower and deeper, respectively, due to the synergistic effect between $\Delta\varepsilon^a_\alpha$(q/q') and $\Delta\varepsilon_{\rm VBM}$, as shown in Fig. 1. In addition, we emphasize that for some unconventional band-edge changes different from type-I and type-II cases, similar analysis can be made to reach the exact rules.

C. Verification in GaN

Taking GaN as a prototype example, we have systematically studied the effects of temperature on ε_α(q/q') for ten different defects (see Appendix D for computational details). The donorlike defects include *N* vacancy (V_N), substitutional Si_{Ga}, Ge_{Ga}, and O_N, while the acceptorlike defects include Mg_{Ga}, Zn_{Ga}, Be_{Ga}, Ca_{Ga}, Cd_{Ga}, and C_N [39,40]. Many of them are commonly observed in GaN [39,40].

First, we test the relationship between ΔF^{el} and $\delta V_{q\to q'}$ in GaN. As shown in Fig. 2(a), the calculated ΔF^{el} and ΔE^{th} for these defects are almost identical, except for Si_{Ga} and O_N between 0 and +1 charge-state transitions at $T > 800$ K, confirming that the contributions of E^{el} and S^{el} to F^{el} are usually small in semiconductors [12,31]. Deviations at high temperatures partially originate from the shallow-level-induced electron-occupation changes. E^{th} can be directly evaluated using first-principles calculations under hydrostatic-stress conditions [41,42], adopting the experimental φ_V [43]. As shown in Fig. 2(a), the calculated ΔE^{th} of these defects increase almost linearly as temperature increases. Interestingly, the calculated $\delta V_{q\to q'}$ are all positive for the acceptors during ionization, resulting in the negative ΔE^{th}; the calculated $\delta V_{q\to q'}$ are all negative for the donors during ionization, resulting in the positive ΔE^{th}. Taking 800 K as a typical temperature, as shown in Fig. 2(b), we have plotted the relationship between ΔE^{th} and $\delta V_{q\to q'}$ for these defects, which exhibits an almost linear dependence, confirming our expectation from Eq. (3). A similar linear dependence behavior with different slopes is observed at other temperatures (Fig. S1 [44]).

It is interesting to understand the origin of the diverse $\delta V_{q\to q'}$ values for different defects. Overall, we discover that while $\delta V_{q\to q'}$ is mainly determined by the change of LEO, the LLR can effectively compensate the LEO-induced $|\delta V_{q\to q'}|$; the larger the LLR, the smaller the $|\delta V_{q\to q'}|$. For example, as shown in Fig. 2(b), all donors have a similar $\delta V_{0\to+1} \sim -12$ Å^3 except V_N. The $\delta V_{q\to q'}$ of V_N are q/q' dependent, e.g., $\delta V_{0\to+1} \sim -6$ Å^3 and $\delta V_{+1\to+3} \sim -1$ Å^3. Meanwhile, all the acceptors have similar $\delta V_{0\to-1} \sim +6$ Å^3 expect Mg_{Ga} ($\sim +4.8$ Å^3) and Be_{Ga} ($\sim +2.3$ Å^3). Overall, $\delta V_{q\to q'}$ is mainly determined by the change of LEO around the defect, i.e., the increased LEO always significantly increases the local volume around a defect [28], leading to a positive $\delta V_{q\to q'}$, and the decreased LEO always significantly decreases the local volume around a defect [28], leading to a negative $\delta V_{q\to q'}$. Furthermore, the $\delta V_{q\to q'}$ value also depends on the strength of LLR around the defect. For example, for Si_{Ga}, there is a negligible LLR during the ionization (Fig. S2 [44]), therefore, the large $\delta V_{0\to+1} \sim -12$ Å^3 is mainly induced by the decreased LEO around Si_{Ga}. The cases of Ge_{Ga} and O_N are similar to that of Si_{Ga}, resulting in similar $\delta V_{0\to+1}$ values. For V_N, due to the broken ionic bonds around V_N, the extra electrons from the dangling bonds (DBs) are strongly localized around V_N [up inset, Fig. 2(b)]. During the ionization from 0 to +1, the DB electrons could be partially compensated, which consequently reduces electron screening and enhances Coulomb repulsion

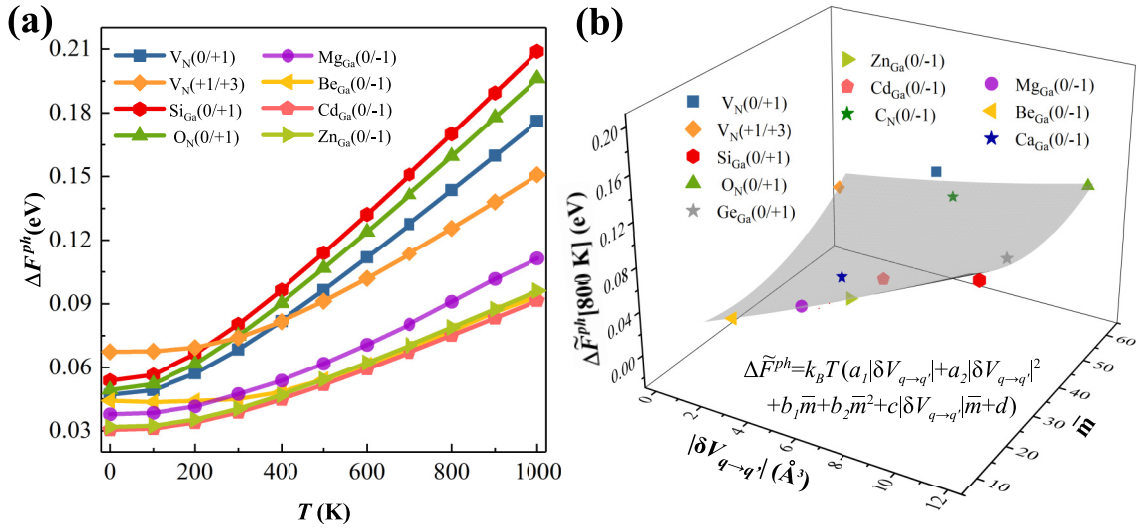

FIG. 3. Vibrational contribution to the temperature dependence of ε_α(q/q') in GaN. (a) ΔF^{ph} as a function of temperature for different defects in GaN. (b) Relationship between $\Delta\widetilde{F}^{ph}$, $|\delta V_{q\to q'}|$ and $\bar{m}$, which can be described by a general polynomial formula. At 800 K, a_1=0.15, a_2=0.0017, $b_1 = -0.0263$, $b_2 = 0.0006$, $c = -0.0019$, and $d = 0.4311$.

between the neighboring Ga^{+3} ions around V_N. As a result, the large LLR effect around V_N (Fig. S3 [44]) effectively expands the local volume and partially compensates the initial local volume shrinkage induced by the decreased LEO. Therefore, the $\delta V_{0\to+1}$ of V_N is significantly smaller than that of Si_{Ga}. In a similar way, the $\delta V_{+1\to+3}$ of V_N can be further reduced from -6 to -1 Å^3, due to the further enhanced LLR effect (Fig. S3 [44]).

Similar to Si_{Ga}, a negligible LLR also exists in acceptors such as Zn_{Ga}, C_N, Ca_{Ga}, and Cd_{Ga} (Fig. S4 [44]). As a result, the increased LEO gives rise to a large $\delta V_{0\to-1}$ ~+6 Å^3 for these acceptors. However, for Be_{Ga}, the smaller atomic size of Be compared to Ga induces one broken ionic bond around Be_{Ga} along the c direction, resulting in a DB hole on the broken *N* bond [bottom inset, Fig. 2(b)] [45]. During the ionization, the DB hole is fully compensated, resulting in a strongly enhanced Coulomb attraction that restores the Be–N bond along the c direction and shrinks the local volume around Be_{Ga} (Fig. S5 [44]). This large local volume shrinkage induced by the LLR effect largely compensates the initial local volume expansion induced by the increased LEO. Hence, compared to Cd_{Ga}, the $\delta V_{0\to-1}$ of Be_{Ga} is reduced to +2.3 Å^3. The strength of LLR in Mg_{Ga} (Fig. S6 [44]) is between Be_{Ga} and Cd_{Ga}, resulting in an intermediate $\delta V_{0\to-1}$ value between that of Be_{Ga} and Cd_{Ga}. Therefore, as shown in Fig. 2(b), we conclude that the variable $\delta V_{q\to q'}$ in different defects are mainly determined by the competing effect between LEO and LLR.

Second, we explore the relationship between ΔF^{ph} and $\delta V_{q\to q'}$ in GaN. As shown in Fig. 3(a), the ΔF^{ph} of both donors and acceptors are positive and increase with increasing temperature. Indeed, F^{ph} includes two parts, i.e., $\Delta F^{ph} = \Delta F^{zp} + \Delta\widetilde{F}^{ph}$. ΔF^{zp} is the contribution of zero-point vibrations and mainly influenced by $\bar{m}$, the larger the $\bar{m}$, the smaller the ΔF^{zp} whereas $\Delta\widetilde{F}^{ph}$ determines the temperature dependence of ΔF^{ph} and we expect that $|\delta V_{q\to q'}|$ and $\bar{m}$ are the two main factors in determining $\Delta\widetilde{F}^{ph}$. Indeed, the $\Delta\widetilde{F}^{ph}$ values of all the defects at different temperatures can be well fitted by a simple but unified formula given as

$$\Delta\widetilde{F}^{ph} = k_BT\,(a_1|\delta V_{q\to q'}| + a_2|\delta V_{q\to q'}|^2 + b_1\bar{m} + b_2\bar{m}^2 + c|\delta V_{q\to q'}|\bar{m} + d). \quad (5)$$

Figure 3(b) shows the case of T = 800 K. Similar behaviors are observed at other temperatures but with different parameter values (Fig. S7 [44]). Overall, it is found that the $|\delta V_{q\to q'}|$ term is the dominant factor for $\Delta\widetilde{F}^{ph}$, and a larger $|\delta V_{q\to q'}|$ usually gives a larger $\Delta\widetilde{F}^{ph}$. For example, the larger $\Delta\widetilde{F}^{ph}$ of Si_{Ga} compared to Cd_{Ga} (116 versus 44 meV) is mainly due to its larger $|\delta V_{q\to q'}|$ (~12 versus ~6 Å^3). For defects with similar $|\delta V_{q\to q'}|$ values, $\bar{m}$ becomes important in determining $\Delta\widetilde{F}^{ph}$, and a smaller $\bar{m}$ gives a larger $\Delta\widetilde{F}^{ph}$. For example, comparing Ca_{Ga}, Zn_{Ga}, and Cd_{Ga}, which have a similar $|\delta V_{q\to q'}|$ ~ 6 Å^3, Ca_{Ga} with smaller $\bar{m}$ (19.2) than Zn_{Ga} (24.2) and Cd_{Ga} (33.6) has larger $\Delta\widetilde{F}^{ph}$ (80 meV) compared to Zn_{Ga} (47 meV) and Cd_{Ga} (44 meV). We notice that the calculated $\Delta\widetilde{F}^{ph}$ value for C_N at 600 K also agrees with a previous study [46]. We would like to emphasize that although the fitting parameters may vary if more different defects in GaN are included or if the host is changed to another material, the general formula expressed in Eq. (5) should be valid because it is expected that $\delta V_{q\to q'}$ of defects play a dominated role in determining the $\Delta\widetilde{F}^{ph}$. Moreover, as shown in Fig. 3(a), it is interesting to see the competing effects from $\bar{m}$ (mainly affects ΔF^{zp}) and $\delta V_{q\to q'}$ (mainly determines $\Delta\widetilde{F}^{ph}$) that can make the realigning of ΔF^{ph} of different defects at different temperatures. For example, at lower temperatures, Be_{Ga} has a higher ΔF^{ph} than Mg_{Ga} due to smaller $\bar{m}$; while at higher temperatures, the increased $\Delta\widetilde{F}^{ph}$ makes Mg_{Ga} have higher ΔF^{ph} instead due to its larger $\delta V_{q\to q'}$. Similar analysis are also valid for the cases of $V_N(+1/+3)$ and $O_N(0/+1)$.

Combining the results of ΔF^{el} [Fig. 2(a)] and ΔF^{ph} [Fig. 3(a)], we arrive at the temperature-dependent ε_α(q/q') of defects in GaN. GaN is a type-I semiconductor [33],

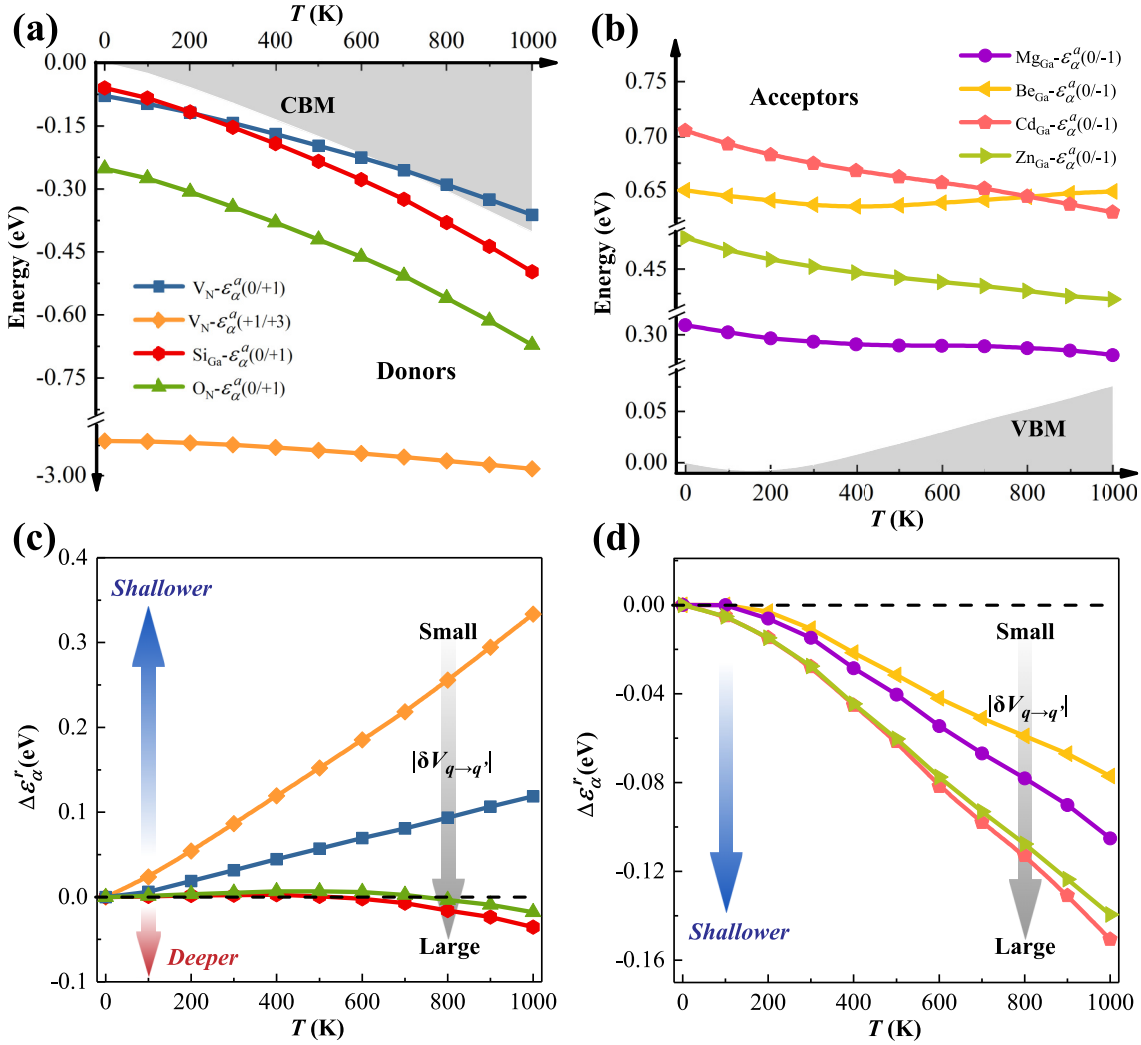

FIG. 4. Temperature dependence of ε_α(q/q') in GaN. ε^a_α(q/q') levels of several typical (a) donors and (b) acceptors in GaN as a function of temperature. Calculated temperature-dependent CBM and VBM changes are also plotted in (a) and (b), respectively. (c) and (d) are corresponding $\Delta\varepsilon^r_\alpha$(q/q') for (a) and (b), respectively. Gray arrow indicates the trend of the sizes of $|\delta V_{q\to q'}|$.

whose $|\Delta\varepsilon_{\rm CBM}|$ [Fig. 4(a)] is noticeably larger than $|\Delta\varepsilon_{\rm VBM}|$ [Fig. 4(b)] at a given temperature, due to the different band-edge orbital characters [33,47]. Importantly, the calculated band gap of GaN as a function of temperature agrees well with the experimental measurements [34], confirming the reliability of our computational methods (Fig. S8 [44]).

As shown in Fig. 4(a), three typical donors, i.e., V_N, Si_{Ga}, and O_N, are selected to demonstrate the temperature dependence of ε_α(q/q') for donors, to verify our proposed rules I(a) and II(a). Interestingly, these donors exhibit quite different temperature-dependent behaviors. Without the consideration of $\Delta\varepsilon_{\rm VBM}$, the ε^a_α(q/q') of all the donors become deeper as the temperature increases, i.e., the higher the temperature, the deeper the ε^a_α(q/q'). Surprisingly, the $\varepsilon^a_\alpha(0/+1)$ of Si_{Ga} and V_N, which have similar shallow levels at T = 0 K (with the inclusion of ΔF^{zp} contribution), exhibit dramatically different temperature dependencies, i.e., the change of $\Delta\varepsilon^a_\alpha(0/+1)$ in Si_{Ga} (−0.44 eV) in the range 0 < T < 1000 K is much larger than that in V_N (−0.28 eV), due to the significantly larger $|\delta V_{0\to+1}|$ in Si_{Ga} [Fig. 2(b)]. Interestingly, although the $\varepsilon^a_\alpha(0/+1)$ of O_N is much deeper than that of Si_{Ga} at 0 K, they exhibit almost the same trend of $\Delta\varepsilon^a_\alpha(0/+1)$ under different temperatures due to their similar $|\delta V_{0\to+1}|$ (the slight difference at high temperatures is caused by their different $\bar{m}$). Unexpectedly, the $\Delta\varepsilon^a_\alpha$(q/q') of one defect can also exhibit totally different behaviors under different charge-state transitions. For example, $\Delta\varepsilon^a_\alpha(0/+1)$ and $\Delta\varepsilon^a_\alpha(+1/+3)$ for V_N are dramatically different because of their largely different $|\delta V_{q\to q'}|$ [Fig. 2(b)]. The above observations, along with other calculated donors (Fig. S9a [44]), confirm the proposed rule I(a) on the relationship between $|\delta V_{q\to q'}|$ and $\Delta\varepsilon^a_\alpha$(q/q') for donors at different temperatures.

Combining ε^a_α(q/q') with the calculated CBM bowing of GaN, we obtain the ε^r_α(q/q') of donors. Interestingly, as exhibited in Fig. 4(c), ε^r_α(q/q') can become either shallower [ε^r_α(q/q') > 0], deeper [ε^r_α(q/q') < 0], or even unchanged [ε^r_α(q/q')∼0] for different donors in different temperature regions. For examples, for Si_{Ga} and O_N, $\Delta\varepsilon^r_\alpha(0/+1) \approx 0$ in the range 0 < T < 500 K, due to the largest opposing effect between $|\Delta\varepsilon_{\rm CBM}|$ and $|\Delta\varepsilon^a_\alpha(0/+1)|$ [$|\Delta\varepsilon_{\rm CBM}| \approx |\Delta\varepsilon^a_\alpha(0/+1)|$]; for T > 500 K, $|\Delta\varepsilon_{\rm CBM}| < |\Delta\varepsilon^a_\alpha(0/+1)|$ gives rise to $\Delta\varepsilon^r_\alpha(0/+1) < 0$, e.g., $\Delta\varepsilon^r_\alpha(0/+1)$ of Si_{Ga} is −0.04 eV

at T = 1000 K. For V_N, $|\Delta\varepsilon_{CBM}| > |\Delta\varepsilon^a_\alpha(0/+1)|$ in the range $0 < T < 1000$ K, resulting in $\Delta\varepsilon^r_\alpha(q/q') > 0$. Among all the $\Delta\varepsilon^r_\alpha(q/q')$, the largest value occurs in the $\Delta\varepsilon^r_\alpha(+1/+3)$ of V_N (0.33 eV at T = 1000 K), due to the smallest opposing effect between $|\Delta\varepsilon_{CBM}|$ and $|\Delta\varepsilon^a_\alpha(+1/+3)|$. The above observations, along with other calculated donors (Fig. S9a [44]), confirm our proposed rule II(a) that the $\Delta\varepsilon^r_\alpha(q/q')$ of donors in type-I semiconductors is determined by the relative magnitude and sign of $\Delta\varepsilon^a_\alpha(q/q')$ and $\Delta\varepsilon_{CBM}$.

In Fig. 4(b), four typical acceptors, i.e., Zn_{Ga}, Mg_{Ga}, Be_{Ga}, and Cd_{Ga}, are selected to demonstrate the temperature dependence of $\varepsilon_\alpha(q/q')$ for acceptors, to verify our proposed rules I(b) and II(b). Holding large $|\delta V_{0\to-1}|$, the $\varepsilon^a_\alpha(0/-1)$ of Cd_{Ga} and Zn_{Ga} always becomes shallower [i.e., $\varepsilon^a_\alpha(0/-1) < 0$] as temperature increases. Interestingly, regardless of the significantly different $\varepsilon^a_\alpha(0/-1)$ values at 0 K for Cd_{Ga} and Zn_{Ga}, their $\Delta\varepsilon^a_\alpha(0/-1)$ exhibit similar temperature dependences, mostly due to their similar $|\delta V_{0\to-1}|$ [Fig. 2(b)]. Again, their slightly different $\Delta\varepsilon^a_\alpha(0/-1)$ at high temperatures could be due to their different $\bar{m}$. Surprisingly, although the Cd_{Ga} and Be_{Ga} have close $\varepsilon^a_\alpha(0/-1)$ values at 0 K, their $\Delta\varepsilon^a_\alpha(0/-1)$ exhibit different (even opposite) temperature dependencies due to their significantly different $|\delta V_{0\to-1}|$]Fig. 2(b)]; with small $|\delta V_{0\to-1}|$, the $\varepsilon^a_\alpha(0/-1)$ of Be_{Ga} becomes even deeper when T > 400 K, swapping the relative positions of Cd_{Ga} and Be_{Ga} at T = 0 K and T = 1000 K. Since the $|\delta V_{0\to-1}|$ of Mg_{Ga} is in between Cd_{Ga} and Be_{Ga}, the $\Delta\varepsilon^a_\alpha(0/-1)$ of Mg_{Ga} is ~ 0 in the range $300 < T < 700$ K. These observations, along with other calculated acceptors (Fig. S9b [44]), confirm rule I(b) on the $\Delta\varepsilon^a_\alpha(q/q')$ of acceptors, especially the critical role played by $|\delta V_{q\to q'}|$. We emphasize that the values of $|\Delta\varepsilon^a_\alpha(q/q')|$ for acceptors are usually much smaller than those for donors, due to the large canceling effect between ΔF^{el} and ΔF^{ph} for acceptors.

Combining $\varepsilon^a_\alpha(q/q')$ with the calculated VBM bowing of GaN, we can obtain the $\varepsilon^r_\alpha(q/q')$ of acceptors. Overall, as shown in Fig. 4(d), the $\varepsilon^r_\alpha(0/-1)$ of all acceptors in GaN becomes shallower [i.e., $\Delta\varepsilon^r_\alpha(0/-1) < 0$]. For Cd_{Ga} and Zn_{Ga}, the synergistic effect between $\Delta\varepsilon^a_\alpha(0/-1)$ and $\Delta\varepsilon_{VBM}$ results in a large value of $\Delta\varepsilon^r_\alpha(0/-1)$, e.g., $\Delta\varepsilon^r_\alpha(0/-1) = -0.15$ eV at T = 1000 K. For Mg_{Ga} with $\Delta\varepsilon^a_\alpha(0/-1) \sim 0$, its $\Delta\varepsilon^r_\alpha(0/-1)$ closely follows the trend of $\Delta\varepsilon_{VBM}$. For Be_{Ga}, the opposing effect between $\Delta\varepsilon^a_\alpha(0/-1)$ and $\Delta\varepsilon_{VBM}$ leads to a small $\Delta\varepsilon^r_\alpha(0/-1)$. The above observations, along with other calculated acceptors (Fig. S9b [44]), confirm our proposed rule II(b) that the $\varepsilon^r_\alpha(q/q')$ of acceptors in type-I semiconductors, depending on the size of $|\delta V_{q\to q'}|$, can exhibit either synergistic or opposing effects between $\varepsilon^a_\alpha(q/q')$ and $\Delta\varepsilon_{VBM}$.

III. OUTLOOK AND CONCLUSION

We emphasize that although the overall sizes of $|\Delta\varepsilon_\alpha(q/q')|$ are not huge in GaN (generally <0.4 eV), we expect that the temperature effect, obeying the same rules as we have developed, could be much more noticeable in many other systems, e.g., superhard semiconductors (e.g., diamond, in which defects play a key role for realizing quantum bits) or organic-inorganic hybrid perovskites (e.g., $MAPbI_3$, in which defects play a key role for limiting their solar efficiencies), in which the phonon vibrations or band-edge changes are much more significant than those in GaN. Since the carrier concentrations and defect-mediated nonradiative carrier recombinations in semiconductors are very sensitive to the positions of $\varepsilon_\alpha(q/q')$ inside the band gap that are temperature dependent, our theory may also be applied to reexamine or explain many existing puzzles on the disagreements between experimental measurements and static first-principles calculations in the future.

In conclusion, we have derived the basic formulas and consequently established two fundamental rules for the temperature dependence of $\varepsilon_\alpha(q/q')$ for both donors and acceptors in semiconductors, a question that has remained unanswered for decades. As we demonstrated in GaN, the temperature-driven changes of $\varepsilon_\alpha(q/q')$ for different defects can be rather diverse, i.e., they can become shallower, deeper, or stay unchanged. The ultimate behavior is mainly determined by the synergistic or opposing effects between free-energy corrections and band-edge changes. In particular, we discover a previously ignored physical quantity, $\delta V_{q\to q'}$, that plays an unexpectedly central role in determining the temperature evolution of $\varepsilon_\alpha(q/q')$. Generally, these basic formulas and fundamental rules may potentially be applied to design novel semiconductor devices operated under high or varying temperatures.

ACKNOWLEDGMENTS

We thank Dr. J. B. Chen and Dr. P. Li for helpful discussions. S.-H.W. and B.H. acknowledge support from the NSFC (Grants No. 11634003 and No. 12088101) and NSAF No. U1930402. S.Q. acknowledges support from the NSFC (Grant No. 12047508) and Chinese Postdoctoral Science Foundation (Grant No. 2021M690329). Y.-N.W. acknowledges support from the Program for Professor of Special Appointment (Eastern Scholar No. TP2019019). B.M. acknowledges support from the Gianna Angelopoulos Programme for Science, Technology, and Innovation and from the Winton Programme for the Physics of Sustainability. Part of the calculations were performed at Tianhe2-JK at Computational Science Research Center.

S.Q. and Y.-N.W. contributed equally to this work.

APPENDIX A: DERIVATION OF $\varepsilon_\alpha(q/q')$ AT FINITE TEMPERATURE

Without the inclusion of temperature effects, the formation energy of a defect α in charge state q is defined as [12–14]

$$\Delta H_f(\alpha, q) = E(\alpha, q) - E(\text{host}) + \sum n_i E(i) + \sum n_i \mu_i + q\varepsilon_{VBM}(\text{host}) + qE_F. \quad \text{(A1)}$$

E(α,q) is the total energy of the supercell with defect α in charge state q whereas E(host) is the total energy of perfect host without defect or impurity. E(i) is the energy of the elemental constituent i at its elemental monomeric phases and μ_i is its chemical potential refer to E(i). n_i is the number of atoms exchanged with the external environment during the formation of defects for element i, and the charge state q is the number of electrons transferred from the supercell to the reservoirs. ε_{VBM}(host) is the VBM of the host material and E_F is the Fermi energy referring to ε_{VBM}(host).

The ε_α(q/q') is the Fermi level at which the charge state q has the same formation energy with q':

$$\varepsilon_\alpha(q/q')_{w.o.T} = \frac{E(\alpha, q') - E(\alpha, q)}{q - q'} - \varepsilon_{\mathrm{VBM}}(\mathrm{host}). \quad \text{(A2)}$$

With the inclusion of temperature effects, the $\Delta H_f(\alpha,q)$ in Eq. (A1) is replaced by the Gibbs free energy $\Delta G_f(\alpha,q)$, and the $E(\alpha,q)$ [$E(\alpha,q')$] is replaced by free energy $F(\alpha,q)$ [$F(\alpha,q')$],

$$\begin{aligned}\Delta G_f(\alpha, q)[P, T] = {} & F(\alpha, q)[V, T] - F(\mathrm{host})[V_{\mathrm{host}}, T] \\ & + (V - V_{\mathrm{host}})P + \sum n_i F(i)[V_i, T] \\ & + \sum n_i \mu_i[P, T] + q\varepsilon_{\mathrm{VBM}}(\mathrm{host})[V_{\mathrm{host}}, T] \\ & + qE_F[V, T], \end{aligned} \quad \text{(A3)}$$

where P and T are the pressure and temperature, respectively. V and V_{host} are the volumes of the system with defects and the host system under pressure P, respectively. In our case of no external pressure (P = 0), Eq. (A3) can be written as

$$\begin{aligned}\Delta G_f(\alpha, q)[P, T] = {} & F(\alpha, q)[V, T] - F(\mathrm{host})[V, T] \\ & + \sum n_i F(i)[V_i, T] \\ & + \sum n_i \mu_i[P, T] + q\varepsilon_{\mathrm{VBM}}(\mathrm{host})[V, T] \\ & + qE_F[V, T]. \end{aligned} \quad \text{(A4)}$$

Accordingly, with the inclusion of temperature effects, ε_α(q/q') is given by

$$\begin{aligned}\varepsilon_\alpha(q/q')[V, T] = {} & \frac{F(\alpha, q')[V, T] - F(\alpha, q)[V, T]}{q - q'} \\ & - \varepsilon_{\mathrm{VBM}}(\mathrm{host})[V, T]. \end{aligned} \quad \text{(A5)}$$

The free energy F can be expanded around the equilibrium position as

$$F(\{\mathbf{R}_I\}) = F_0 + \frac{1}{2}\sum_{k,l} u_k u_l \left[\frac{\partial^2 F}{\partial R_k \partial R_l}\right]_{\{\mathbf{R}_I^0\}} + O(u^3), \quad \text{(A6)}$$

where R_I are the atomic coordinates of atom I, and R_I^0 are the equilibrium position. u_k, defined as R_k-R_k^0, are the atomic displacements of atom k from the equilibrium positions. The first and second terms are the electron and phonon free energies, respectively. Accordingly, F_0 includes two parts, E (the total energy of the system without the consideration of temperature effects) and F^{el} (the corrections of the free energy induced by the electron contribution). Ignoring high order terms, we have

$$F[V, T] = E + F^{\mathrm{el}}[V, T] + F^{\mathrm{ph}}[V, T], \quad \text{(A7)}$$

where F^{ph} is the correction of the free energy induced by the phonon vibration.

Under the QHA, F^{el} can be written as [13,29,30]

$$F^{\mathrm{el}}[V, T] = E^{\mathrm{th}}[V, T] + E^{\mathrm{el}}[V, T] - TS^{\mathrm{el}}[V, T]. \quad \text{(A8)}$$

Here, E^{th} is purely the internal energies of the expanded lattice at finite temperature. The latter two terms come from the Fermi-Dirac distribution of the electronic eigenstates at finite temperature, which slightly affect the occupations of each eigenstate. Accordingly, E^{el} is the energy correction of eigenvalue summation induced by temperature dependence of the occupation of KS energy levels from Fermi-Dirac distribution and S^{el} is the entropy induced by the disorder of the partial occupation. For metal, because the density of states (DOS) is nonzero at the Fermi level, the temperature dependence of the occupation of eigenstates can be significant and the contributions from E^{el} and S^{el} are important. On the contrary, for semiconductors (especially WBG semiconductors), the temperature dependence of the occupation of eigenstates is negligible and so are the contributions from E^{el} and S^{el}, as also verified in our calculations [Fig. 2(a)]. Therefore, we focus on the E^{th} term in F^{el}.

Under the QHA, F^{ph} can be written as [32]

$$F^{\mathrm{ph}} = \sum_i \left[\frac{1}{2}\hbar\omega_i + k_B T\, ln\left\{1 - \exp\left(-\frac{\hbar\omega_i}{k_B T}\right)\right\}\right], \quad \text{(A9)}$$

where $\hbar$, ω_i, and k_B are the reduced Planck's constant, phonon eigenfrequency, and Boltzmann constant, respectively.

Combining Eq. (A6) to Eq. (A9), we can obtain the ε_α(q/q') of defects under different temperatures:

$$\begin{aligned}\varepsilon_\alpha(q/q')[V, T] = {} & \varepsilon_\alpha(q/q')_{\mathrm{w.o.T}} + \frac{\Delta F^{\mathrm{el}}[V, T] + \Delta F^{\mathrm{ph}}[V, T]}{q - q'} \\ & - \Delta\varepsilon_{\mathrm{VBM}}(host)[V, T]. \end{aligned} \quad \text{(A10)}$$

The second term of Eq. (A10) represents the correction on the free-energy differences between the q and q' configurations induced by the electronic (ΔF^{el}) and vibrational (ΔF^{ph}) contributions. The third term of Eq. (A10) represents the correction on the VBM energy position induced by thermal expansion and electron-phonon coupling ($\Delta\varepsilon_{\mathrm{VBM}} = \Delta\varepsilon^{\mathrm{th}}{}_{\mathrm{VBM}} + \Delta\varepsilon^{\mathrm{ph}}_{\mathrm{VBM}}$).

Without consideration of the external pressure, volume expansion induced by rising temperature can be described by the thermal expansion coefficient. From the definition of the mean volumetric thermal expansion coefficient, we can obtain that T and V are correlated by [48]

$$V = \varphi_V\, T\, V_0 + V_0, \quad \text{(A11)}$$

where φ_V is the mean volumetric thermal expansion coefficient and V_0 is the equilibrium volume of the system at 0 K. Thus, in the case of no external pressure, we can keep T as the only variable in our formula, and the ε_α(q/q') at a finite temperature becomes

$$\begin{aligned}\varepsilon_\alpha(q/q')[T] = {} & \varepsilon_\alpha(q/q')_{\mathrm{w.o.T}} + \frac{\Delta F^{\mathrm{el}}[T] + \Delta F^{\mathrm{ph}}[T]}{q - q'} \\ & - \Delta\varepsilon_{\mathrm{VBM}}(\mathrm{host})[T]. \end{aligned} \quad \text{(A12)}$$

At a given temperature, ΔF^{el}(ΔE^{th}) and $\Delta\varepsilon^{\mathrm{th}}{}_{\mathrm{VBM}}$ can be directly calculated via first-principles calculations under hydrostatic-stress conditions [41,42] (it is noted that the lattice constant after thermal expansion is determined by the experiment thermal expansion coefficients of GaN [43]), ΔF^{ph} can be determined through Eq. (A9) and the calculations of phonon eigenfrequencies for charge states q and q'. Finally, $\Delta\varepsilon^{\mathrm{ph}}_{\mathrm{VBM}}$ can be calculated using the finite displacement approach based on thermal lines [49,50]. Unlike the conventional finite-displacement approach that evaluates each

phonon separately and sum over all phonons, this stochastic approach considers all phonon modes at the same time, and the electron-phonon interaction can be calculated accurately and efficiently.

APPENDIX B: DERIVATION OF ΔE^{th}

Under the QHA, the thermal expansion induced energy correction E^{th} can be treated as arising from strain [41,42]. Therefore, the corrections on the total energy differences between the system with and without defect α induced by the thermal expansion can be written as [28]

$$E^{th}(\alpha, q)[V] - E^{th}(\text{host})[V] = -2\gamma_0\,\Delta V_q[V - V_0(\text{host})] + \Delta\gamma[V - V_0(\text{host})]^2. \quad \text{(B1)}$$

γ_0 is the elastic constant of the host and $\Delta\gamma$ is the change of γ_0 induced by a defect α in charge state q. $\Delta V_q = V_0(\alpha,q) - V_0(\text{host})$ is the volume change induced by the defect α at 0 K, in which $V_0(\text{host})$ and $V_0(\alpha,q)$ are the equilibrium volume of the system without and with defect at 0 K.

We assume that in a large system, a single defect cannot strongly influence the elastic constant, i.e., $\Delta\gamma = 0$ as a first-order approximation, and ΔE^{th} between the two charge states q and q' with the same defect α is

$$\Delta E^{th}(\alpha, q/q')[V] = E^{th}(\alpha, q')[V] - E^{th}(\alpha, q)[V] = -2\gamma_0\,[V - V_0(\text{host})]\,\delta V_{q\to q'}, \quad \text{(B2)}$$

where $\delta V_{q\to q'} = V_0(\alpha,q') - V_0(\alpha,q)$ is the volume change induced by defect α at 0 K when the charge-state changes from q to q'. Combining Eq. (A11), we have

$$\Delta E^{th} = -2\gamma_0\,[V - V_0(\text{host})]\,\delta V_{q\to q'} = -2\gamma_0\,\varphi_V T\,V_0(\text{host})\,\delta V_{q\to q'}. \quad \text{(B3)}$$

APPENDIX C: DERIVATION OF ΔF^{ph}

The phonon contribution to the free energy, F^{ph}, can be described by Eq. (A9). Considering the first-order approximation of the Taylor expansion $e^x = 1+x+x^2/2!+x^3/3!+...$, we have

$$F^{ph}[T] = \sum_i \left[\frac{1}{2}\hbar\omega_i + k_B T \ln\left(\frac{\hbar\omega_i}{k_B T}\right)\right]. \quad \text{(C1)}$$

The ΔF^{ph} between the two charge states q and q' with the same defect α is given by [two states with the same defect have the same number of phonon (i)]

$$\begin{aligned}\Delta F^{ph}(\alpha, q/q')[T] &= F^{ph}(\alpha, q')[T] - F^{ph}(\alpha, q)[T] \\ &= \sum_i \left[\frac{1}{2}\hbar\omega_i(\alpha, q') + k_B T \ln\left(\frac{\hbar\omega_i(\alpha, q')}{k_B T}\right)\right] \\ &\quad - \sum_i \left[\frac{1}{2}\hbar\omega_i(\alpha, q) + k_B T \ln\left(\frac{\hbar\omega_i(\alpha, q)}{k_B T}\right)\right] \\ &= \sum_i \left\{\frac{1}{2}\hbar[\omega_i(\alpha, q') - \omega_i(\alpha, q)] + k_B T \ln\left[\frac{\omega_i(\alpha, q')}{\omega_i(\alpha, q)}\right]\right\}. \end{aligned} \quad \text{(C2)}$$

Defining $\Delta\omega_i = \omega_i(\alpha,q')-\omega_i(\alpha,q)$ and considering the first-order approximation of the Taylor expansion $\ln(1+x)=x-x^2/2+x^3/3-...$, we have

$$\begin{aligned}\Delta F^{ph}(\alpha, q/q')[T] &= \sum_i \left\{\frac{1}{2}\hbar\Delta\omega_i + k_B T \ln\left[1 + \frac{\Delta\omega_i}{\omega_i(\alpha, q)}\right]\right\} \\ &= \sum_i \left[\frac{1}{2}\hbar\Delta\omega_i + k_B T \frac{\Delta\omega_i}{\omega_i(\alpha, q)}\right]. \end{aligned} \quad \text{(C3)}$$

APPENDIX D: COMPUTATIONAL METHODS

1. Parameters of DFT calculations

Within the framework of density functional theory, the first-principles calculations are performed using the VIENNA AB INITIO SIMULATION PACKAGE [51–54]. The projector augmented wave method [55] has been employed to describe the ion-electron interaction, and the atomic coordinates have been relaxed until the atomic forces are less than 0.01 eV/Å. The Heyd-Scuseria-Ernzerhof (HSE06) hybrid functional [56] with the Hartree-Fock exchange parameter $\alpha = 0.31$ is adopted. The optimized lattice constants (a = 3.20 Å and c = 5.20 Å) and the calculated band gap (3.49 eV) of GaN are in good agreement with the experimental values [57,58]. A 96-atom supercell is selected and the spin polarization is considered for all the defects. A 520 eV plane-wave basis cutoff, a Γ-centered 2 ×2 × 2 Monkhorst-Pack k mesh, and a 10^{-5} eV convergence criteria for the total energy are used in our calculations.

For the convergence tests of the phonon calculations, taking Be_{Ga} as an example, the ΔF^{ph} of Be_{Ga} with different parameters are calculated. To reduce the computational cost, the Perdew-Burke-Ernzerhof functional [59] is adopted for the tests. A plane-wave basis cutoff of 520 eV, a Γ-centered Monkhorst-Pack k mesh of 2 × 2× 2 (for a 96 atoms supercell), and a convergence criterion of 10^{-7} eV for the total energy of the electronic self-consistent iterations are selected for the phonon-related calculations. See the test results in Fig. S10 [44]. Moreover, the good agreement of band gap between calculations and experiments, as shown in Fig. S8 [44], demonstrates that $\Delta\varepsilon^{ph}$ is also well converged under these parameters.

2. Supercell size and shape

The convergence tests of the supercell size and shape are also done to make sure the finite-size error can be largely avoided. Different supercell sizes from 72 to 128 atoms and within hexagonal or orthorhombic cells are tested. ΔF^{ph} of these defects have been converged with a negligible error for supercells larger than 96 atoms, regardless of the shape, in agreement with previous calculations [46]. Thus, we selected the 96-atom orthorhombic supercell.

3. Lattice constants in phonon-related calculations

Strictly speaking, GaN crystal expands as temperature increases, so the calculations of phonon modes at finite temperature should be performed based on the expanded GaN lattice. Nonetheless, we find that using the lattice constant decided at 0 K only introduces negligible errors for the phonon modes and ΔF^{ph}, shown as the following test.

Figure S11 [44] shows the DOS of ω_i ($DOS_{ph\omega}$) for Be_{Ga} using the lattice parameters at 0 K and 800 K, respectively. In both Be^{0}_{Ga} and Be^{-1}_{Ga} cases, the DOS of lower frequency states (below the dash line) are almost the same for different temperatures, whereas the higher frequency states (above the dash line) slightly downshift in $DOS_{ph\omega}$ as the lattice expands from 0 K to 800 K. This suggests the impact of thermal expansion on ΔF^{ph} can be neglected because of the same behavior of DOS with different charge states. Our calculation shows that ΔF^{ph} has only 2 meV error when lattice thermal expansion is not considered at 800 K for Be_{Ga} in GaN. According to these tests, we choose the lattice constants of 0 K and neglect the thermal expansion during our phonon-related calculations.

[1] W. S. Yang, B.-W. Park, E. H. Jung, N. J. Jeon, Y. C. Kim, D. U. Lee, S. S. Shin, J. Seo, E. K. Kim, J. H. Noh, and S. I. Seok, Iodide management in formamidinium-lead-halide-based perovskite layers for efficient solar cells, Science **356**, 1376 (2017).

[2] J. Jeong, M. Kim, J. Seo, H. Lu, P. Ahlawat, A. Mishra, Y. Yang, M. A. Hope, F. T. Eickemeyer, M. Kim *et al.*, Pseudo-halide anion engineering for α-$FAPbI_3$ perovskite solar cells, Nature (London) **592**, 381 (2021).

[3] J. Kong, Y. Shin, J. A. Röhr, H. Wang, J. Meng, Y. Wu, A. Katzenberg, G. Kim, D. Y. Kim, T.-D. Li *et al.*, CO_2 doping of organic interlayers for perovskite solar cells, Nature (London) **594**, 51 (2021).

[4] K. Lin, J. Xing, L. N. Quan, F. P. García de Arquer, X. Gong, J. Lu, L. Xie, W. Zhao, D. Zhang, C. Yan *et al.*, Perovskite light-emitting diodes with external quantum efficiency exceeding 20 per cent, Nature (London) **562**, 245 (2018).

[5] J. Luo, X. Wang, S. Li, J. Liu, Y. Guo, G. Niu, L. Yao, Y. Fu, L. Gao, Q. Dong *et al.*, Efficient and stable emission of warm-white light from lead-free halide double perovskites, Nature (London) **563**, 541 (2018).

[6] S.-Y. Xu, Y. Xia, L. A. Wray, S. Jia, F. Meier, J. H. Dil, J. Osterwalder, B. Slomski, A. Bansil, H. Lin *et al.*, Topological phase transition and texture inversion in a tunable topological insulator, Science **332**, 560 (2011).

[7] J. Zhang, C.-Z. Chang, P. Tang, Z. Zhang, X. Feng, K. Li, L. Wang, X. Chen, C. Liu, W. Duan *et al.*, Topology-driven magnetic quantum phase transition in topological insulators, Science **339**, 1582 (2013).

[8] J. L. Collins, A. Tadich, W. Wu, L. C. Gomes, J. N. B. Rodrigues, C. Liu, J. Hellerstedt, H. Ryu, S. Tang, S.-K. Mo *et al.*, Electric-field-tuned topological phase transition in ultrathin Na_3Bi, Nature (London) **564**, 390 (2018).

[9] W. F. Koehl, B. B. Buckley, F. J. Heremans, G. Calusine, and D. D. Awschalom, Room temperature coherent control of defect spin qubits in silicon carbide, Nature (London) **479**, 84 (2011).

[10] Y. He, S. K. Gorman, D. Keith, L. Kranz, J. G. Keizer, and M. Y. Simmons, A two-qubit gate between phosphorus donor electrons in silicon, Nature (London) **571**, 371 (2019).

[11] N. P. de Leon, K. M. Itoh, D. Kim, K. K. Mehta, T. E. Northup, H. Paik, B. S. Palmer, N. Samarth, S. Sangtawesin, and D. W. Steuerman, Materials challenges and opportunities for quantum computing hardware, Science **372**, eabb2823 (2021).

[12] A. Alkauskas, P. Deák, J. Neugebauer, A. Pasqarello, and C. G. Van de Walle, *Advanced Calculations for Defects in Materials: Electronic Structure Methods* (John Wiley & Sons, Weinheim, 2011).

[13] C. Freysoldt, B. Grabowski, T. Hickel, J. Neugebauer, G. Kresse, A. Janotti, and C. G. Van de Walle, First-principles calculations for point defects in solids, Rev. Mod. Phys. **86**, 253 (2014).

[14] A. Zunger, and O. I. Malyi, Understanding doping of quantum materials, Chem. Rev. **121**, 3031 (2021).

[15] K. Carling, G. Wahnström, T. R. Mattsson, A. E. Mattsson, N. Sandberg, and G. Grimvall, Vacancies in Metals: From First-Principles Calculations to Experimental Data, Phys. Rev. Lett. **85**, 3862 (2000).

[16] M. Youssef and B. Yildiz, Intrinsic point-defect equilibria in tetragonal ZrO_2: Density functional theory analysis with finite-temperature effects, Phys. Rev. B **86**, 144109 (2012).

[17] A. Glensk, B. Grabowski, T. Hickel, and J. Neugebauer, Breakdown of the Arrhenius Law in Describing Vacancy Formation Energies: The Importance of Local Anharmonicity Revealed by *Ab Initio* Thermodynamics, Phys. Rev. X **4**, 011018 (2014).

[18] J. B. Casady and R. W. Johnson, Status of silicon carbide (SiC) as a wide-bandgap semiconductor for high-temperature applications: A review, Solid-State Electron. **39**, 1409 (1996).

[19] P. G. Neudeck, R. S. Okojie, and L.-Y. Chen, High-temperature electronics—a role for wide bandgap semiconductors? Proc. IEEE **90**, 1065 (2002).

[20] J. Millán, P. Godignon, X. Perpiñà, A. Pérez-Tomás, and J. Rebollo, A survey of wide band gap power semiconductor devices, IEEE Trans. Power Electron. **29**, 2155 (2014).

[21] T. Harada, S. Ito, and A. Tsukazaki, Electric dipole effect in $PdCoO_2/\beta$-Ga_2O_3 Schottky diodes for high-temperature operation, Sci. Adv. **5**, eaax5733 (2019).

[22] X. Wang, H. Zhang, T. Baba, H. Jiang, C. Liu, Y. Guan, O. Elleuch, T. Kuech, D. Morgan, J.-C. Idrobo *et al.*, Radiation-induced segregation in a ceramic, Nat. Mater. **19**, 992 (2020).

[23] P. L. Dreike, D. M. Fleetwood, D. E. King, D. C. Sprauer, and T. E. Zipperian, An overview of high-temperature electronic device technologies and potential applications, IEEE Trans. Comp., Packag., Manufact. Technol. A **17**, 594 (1994).

[24] D. G. Senesky, B. Jamshidi, K. B. Cheng, and A. P. Pisano, Harsh environment silicon carbide sensors for health and performance monitoring of aerospace systems: A review, IEEE Sens. J. **9**, 1472 (2009).

[25] T. Ghidini, Materials for space exploration and settlement, Nat. Mater. **17**, 846 (2018).

[26] O. Tschauner, S. Huang, E. Greenberg, V. B. Prakapenka, C. Ma, G. R. Rossman, A. H. Shen, D. Zhang, M. Newville, A. Lanzirotti, and K. Tait, Ice-VII inclusions in diamonds: Evidence for aqueous fluid in Earth's deep mantle, Science **359**, 1136 (2018).

[27] B. Monserrat, Electron-phonon coupling from finite differences, J. Phys.: Condens. Matter **30**, 083001 (2018).

[28] X. Yan, P. Li, S.-H. Wei, and B. Huang, Universal theory and basic rules of strain-dependent doping behaviors in semiconductors, Chin. Phys. Lett. **38**, 087103 (2021).

[29] N. D. Mermin, Thermal properties of the inhomogeneous electron gas, Phys. Rev. **137**, A1441 (1965).

[30] Y. Wang, Z. K. Liu, and L. Q. Chen, Thermodynamic properties of Al, Ni, NiAl, and Ni_3Al from first-principles calculations, Acta Mater. **52**, 2665 (2004).

[31] S. Baroni, S. de Gironcoli, A. Dal Corso, and P. Giannozzi, Phonons and related crystal properties from density-functional perturbation theory, Rev. Mod. Phys. **73**, 515 (2001).

[32] D. C. Wallace, *Thermodynamics of Crystals* (Dover, New York, 1998).

[33] E. Zdanowicz, P. Ciechanowicz, K. Opolczynska, D. Majchrzak, J.-G. Rousset, E. Piskorska-Hommel, M. Grodzicki, K. Komorowska, J. Serafinczuk, D. Hommel, and R. Kudrawiec, As-related stability of the band gap temperature dependence in N-rich GaNAs, Appl. Phys. Lett. **115**, 092106 (2019).

[34] K. B. Nam, J. Li, J. Y. Lin, and H. X. Jiang, Optical properties of AlN and GaN in elevated temperatures, Appl. Phys. Lett. **85**, 3489 (2004).

[35] Y. P. Varshni, Temperature dependence of the energy gap in semiconductors, Physica **34**, 149 (1967).

[36] R. Saran, A. Heuer-Jungemann, A. G. Kanaras, and R. J. Curry, Giant bandgap renormalization and exciton-phonon scattering in perovskite nanocrystals, Adv. Opt. Mater. **5**, 1700231 (2017).

[37] R. L. Milot, G. E. Eperon, H. J. Snaith, M. B. Johnston, and L. M. Herz, Temperature-dependent charge-carrier dynamics in $CH_3NH_3PbI_3$ Perovskite thin films, Adv. Funct. Mater. **25**, 6218 (2015).

[38] M. Ibrahim Dar, G. Jacopin, S. Meloni, A. Mattoni, N. Arora, A. Boziki, S. M. Zakeeruddin, U. Rothlisberger, and M. Grätzel, Origin of unusual bandgap shift and dual emission in organic-inorganic lead halide perovskites, Sci. Adv. **2**, e1601156 (2016).

[39] C. G. Van de Walle and J. Neugebauer, First-principles calculations for defects and impurities: Applications to III-nitrides, J. Appl. Phys. **95**, 3851 (2004).

[40] M. A. Reshchikov and H. Morkoç, Luminescence properties of defects in GaN, J. Appl. Phys. **97**, 061301 (2005).

[41] A. Togo, L. Chaput, I. Tanaka, and G. Hug, First-principles phonon calculations of thermal expansion in Ti_3SiC_2, Ti_3AlC_2, and Ti_3GeC_2, Phys. Rev. B **81**, 174301 (2010).

[42] A. Togo and I. Tanaka, First principles phonon calculations in materials science, Scr. Mater. **108**, 1 (2015).

[43] H. P. Maruska, and J. J. Tietjen, The preparation and properties of vapor-deposited single-crystalline GaN, Appl. Phys. Lett. **15**, 327 (1969).

[44] See Supplemental Material at http://link.aps.org/supplemental/10.1103/PhysRevB.105.115201 for relationship between the $\delta V_{q\to q'}$ of different defects and the ΔEth at other temperatures (Fig. S1), local crystal structures of different defects in GaN (Figs. S2– S6), relationship between $\Delta\widetilde{F}^{\mathrm{ph}}$, $|\delta V_{q\to q'}|$ and $\bar{m}$ at other temperatures (Fig. S7), comparison of calculated and experimentally measured band gap (E_g) of GaN as a function of temperature (Fig. S8), $\varepsilon_\alpha(q/q')$ levels of typical defects in GaN as a function of temperature (Fig. S9), and calculation convergence tests (Fig. S10).

[45] S. Lany and A. Zunger, Dual nature of acceptors in GaN and ZnO: The curious case of the shallow Mg_{Ga} deep state, Appl. Phys. Lett. **96**, 142114 (2010).

[46] D. Wickramaratne, C. E. Dreyer, B. Monserrat, J.-X. Shen, J. L. Lyons, A. Alkauskas, and C. G. Van de Walle, Defect identification based on first-principles calculations for deep level transient spectroscopy, Appl. Phys. Lett. **113**, 192106 (2018).

[47] Y.-H. Li, X. G. Gong, and S.-H. Wei, *Ab initio* all-electron calculation of absolute volume deformation potentials of IV-IV, III-V, and II-VI semiconductors: The chemical trends, Phys. Rev. B **73**, 245206 (2006).

[48] T. J. Ahrens, *Mineral Physics & Crystallography: A Handbook of Physical Constants* (American Geophysical Union, Washington, 1995).

[49] B. Monserrat, Vibrational averages along thermal lines, Phys. Rev. B **93**, 014302 (2016).

[50] B. Monserrat, Correlation effects on electron-phonon coupling in semiconductors: Many-body theory along thermal lines, Phys. Rev. B **93**, 100301(R) (2016).

[51] G. Kresse and J. Hafner, *Ab initio* molecular dynamics for liquid metals, Phys. Rev. B **47**, 558 (1993).

[52] G. Kresse and J. Hafner, *Ab initio* molecular-dynamics simulation of the liquid-metal-amorphous-semiconductor transition in germanium, Phys. Rev. B **49**, 14251 (1994).

[53] G. Kresse and J. Furthmüller, Efficiency of *ab initio* total energy calculations for metals and semiconductors using a plane-wave basis set, Comput. Mater. Sci. **6**, 15 (1996).

[54] G. Kresse and J. Furthmüller, Efficient iterative schemes for *ab initio* total-energy calculations using a plane-wave basis set, Phys. Rev. B **54**, 11169 (1996).

[55] G. Kresse and D. Joubert, From ultrasoft pseudopotentials to the projector augmented-wave method, Phys. Rev. B **59**, 1758 (1999).

[56] J. Heyd and G. E. Scuseria, Hybrid functionals based on a screened Coulomb potential, J. Chem. Phys. **118**, 8207 (2003).

[57] B. Monemar, Fundamental energy gap of GaN from photoluminescence excitation spectra, Phys. Rev. B **10**, 676 (1974).

[58] O. Madelung, *Semiconductors-Basic Data* (Springer, Berlin, 1996).

[59] J. P. Perdew, K. Burke, and M. Ernzerhof, Generalized Gradient Approximation Made Simple, Phys. Rev. Lett. **77**, 3865 (1996).